Predictor-Controller Approach for Q-Law 6th Element Targeting in Low-Thrust Trajectory Design

Lorenz Veithen[1,2], Maximilian Keller[2]

[1] *Faculty of Aerospace Engineering, Delft University of Technology*
Delft, The Netherlands
Email: lveithen@tudelft.net

[2] *Deutsches Zentrum für Luft- und Raumfahrt e.V.*
Oberpfaffenhofen, Germany
Email: Maximilian.Keller@dlr.de

Abstract – **Electric propulsion enables ambitious and affordable space missions by substantially reducing the fuel mass in comparison to lower specific impulse propulsion. However, the optimisation of the according transfer trajectories is particularly challenging due to their typically low thrust characteristics, resulting in many-revolution transfers with many local minima and highly non-linear dynamics. The Q-Law guidance algorithm can provide near-optimal low-thrust trajectories with minimal computational effort, which can be used either as an initial guess for the optimisation to ensure a faster convergence or directly for mission analysis. In the classical formulation presented by [1] the Q-law does not allow to target a specific position in the final orbit, rendering a poor initial guess in cases where it is a constraint. Such a constraint could be the geographical longitude when acquiring a geostationary orbit, but also the position within a constellation of Low Earth Orbit and Medium Earth Orbit satellites, or within a rendezvous scenario. This study proposes a predictor-controller approach to enable Q-Law targeting capabilities for this fast-moving orbital element in the final orbit, as a generalisation to a method proposed by [2] to target a geographical longitude in geostationary orbit. This work uses the semi-major axis augmented Modified Equinoctial Elements formulation of the Q-law and has been tested for a range of orbital transfers with varying inclinations and eccentricities. A sensitivity analysis on the key parameters of the algorithm, with respect to its convergence, is presented. This approach permits to quickly compute near-optimal transfers to a specified slot in the final orbit.**

I. INTRODUCTION

The first record of the concept of low-thrust Electric Propulsion (EP) for spaceflight trajectories dates back from the early 1900s [3, 4], but its active development only started in 1957 [5]. Since then, its potential to allow for significant mass savings for long-term interplanetary cruise and planetocentric orbital operations has been widely recognised [6, 7]. However, while the optimisation of high thrust chemical propulsion trajectories has been studied in great details [9-13], the optimisation of many-revolutions low-thrust trajectories is significantly more challenging due to the highly nonlinear dynamics, orbital perturbations, and many local minima [14, 15].

Low-thrust transfer optimisation is classically formulated as an Optimal Control Problem (OCP), limited to continuous dynamics with real variables and parameters [14]. However, spacecrafts employing EP often require multiple modes of operations, such as coasting, which introduce discontinuities in the dynamics. This is tackled using phases relative to each operational mode, throughout which the dynamics are continuous. The optimisation is then considered a Hybrid Optimal Control Problem (HOCP). Numerous numerical and analytical methods have been presented in literature based on either the OCP or HOCP formulation [14, 16-19], with most categorised as either direct or indirect techniques, or a hybrid of the two [20, 21]. In the indirect method the necessary conditions for optimality are derived using calculus of variations and the resulting boundary value problem is then solved e.g. numerically via shooting techniques [16]. Conversely, direct methods discretise the optimal control problem first and then solve the resulting Non-Linear Programming problem via gradient-based techniques [16]. This means iterating an appropriate initial guess of optimisation variables such that the objective function is minimised to find the closest local minimum (e.g. using Sequential Quadratic Programming). Therefore, direct methods strongly benefit from an initial guess close to the global optimum. To quickly generate such a near-optimal and physically feasible initial guess, Lyapunov control laws have recently gained in popularity [20, 22].

Lyapunov theory considers the stability of a system based on an indirect or direct method. The latter is particularly of interest as it permits to analyse and design non-linear systems to achieve global stability [23]. The fundamental principle being that if the total energy of the system is continuously dissipating, the system will reach a stable equilibrium point. Therefore, a suitable positive scalar Lyapunov candidate function describing the energy of the system is selected and its first time derivative along the system trajectory is evaluated. In the case of low-thrust trajectory design, the thrust

direction is chosen to ensure a maximum decrease of the Lyapunov function at each step. Reference [24] was the first to employ Keplerian elements in the Lyapunov function and to develop a control law for low-thrust trajectories. Later, [25] presented a candidate function using the angular momentum and eccentricity vectors and solved the trajectory in Cartesian coordinates. Reference [26] developed another Lyapunov function based on the analytic expressions of the maximum rates of change in orbital elements. The latter has been refined and improved over the past two decades and became the preferred option to quickly obtain a reasonable low-thrust transfer trajectory [27, 28].

Several alternative formulations to the candidate function presented by [28] (which uses Keplerian elements), called the proximity quotient or Q-Law, have been proposed in literature. Reference [29] presented a partial formulation making use of the Modified Equinoctial Elements (MEE) and optimised the weights of the law using a Genetic Algorithm (GA). This work was extended by [30] who completed the Q-Law formulation and replaced the semi-latus rectum of the MEE set by the semi-major axis (AMEE). This modification results in a better convergence of the algorithm. However, [31] found that approximations of the maximum rate of change of the f and g elements are inaccurate for significantly eccentric and inclined orbits, requiring to evaluate those values numerically. Furthermore, although those formulations use constant weights, some attempts have been made to use time-varying weights [20, 32, 33].

Although the Q-Law is a powerful tool which has been used for both research and mission design purposes [34, 35], the classical formulation does not permit sixth-element targeting [27], which is necessary for rendezvous missions. Numerous attempts have been made in literature, such as introducing the sixth-element directly in the proximity quotient [36], changing the fast variable to a slow-moving term related to the mean anomaly [36], having a built-in phasing mode (RQ-Law) [31], and augmenting the classical elements [37]. The two first methods fail according to [36], the third one is suboptimal as targeting only starts after the target orbit is reached, and the last method was found to yield inconsistent travel times [36].

This work presents a reliable method to target a specific moving-position in any bounded target orbit based on a predictor-controller approach extending the capabilities of the Q-Law. The algorithm was derived as a generalisation of the Geostationary Orbit (GEO) longitude targeting algorithm from [2] to both circular and eccentric orbits.

II. METHODS

A. Dynamical Framework

The spacecraft is considered as a point mass in the Earth central gravity field, where orbital perturbations were neglected. Therefore, the electric thruster is the only external force acting on the body. The propagation is performed using the Modified Equinoctial Elements (p, f, g, h, k, L) formulation of the perturbation equations [38], which only have a singularity for an inclination of $i = 180°$. However, the true longitude L was used as independent variable to ensure a constant data density throughout the orbit: a constant time step would result in more points around the apocenter than the pericentre for eccentric orbits. The time formulation of the MEE's equations of motion is given by [39],

$$\frac{\mathrm{d}p}{\mathrm{d}t} = \frac{2p}{w}\sqrt{\frac{p}{\mu}}\Delta_t \tag{1}$$

$$\frac{\mathrm{d}f}{\mathrm{d}t} = \sqrt{\frac{p}{\mu}}\Big[\Delta_r \sin L + \big((w+1)\cos L + f\big)\frac{\Delta_t}{w} - (h\sin L - k\cos L)\frac{g\Delta_n}{w}\Big] \tag{2}$$

$$\frac{\mathrm{d}g}{\mathrm{d}t} = \sqrt{\frac{p}{\mu}}\Big[-\Delta_r \cos L + \big((w+1)\sin L + g\big)\frac{\Delta_t}{w} + (h\sin L - k\cos L)\frac{f\Delta_n}{w}\Big] \tag{3}$$

$$\frac{\mathrm{d}h}{\mathrm{d}t} = \sqrt{\frac{p}{\mu}}\frac{s^2\Delta_n}{2w}\cos L \tag{4}$$

$$\frac{\mathrm{d}k}{\mathrm{d}t} = \sqrt{\frac{p}{\mu}}\frac{s^2\Delta_n}{2w}\sin L \tag{5}$$

$$\frac{\mathrm{d}L}{\mathrm{d}t} = \sqrt{\mu p}\left(\frac{w}{p}\right)^2 + \frac{1}{w}\sqrt{\frac{p}{\mu}}(h\sin L - k\cos L)\Delta_n \tag{6}$$

with t the time variable, μ is the central body gravitational parameter, $s^2 = 1 + h^2 + k^2$ and $w = 1 + f\cos L + g\sin L$. The $\Delta_r, \Delta_t, \Delta_n$ perturbing accelerations are expressed in the RTN frame, a spacecraft-centred coordinate system where R is parallel to the position vector, N is in the direction of the angular momentum vector (perpendicular to the orbital plane), and T completes the right-handed coordinate system. The set of equations is completed by (7),

$$\frac{\mathrm{d}m}{\mathrm{d}t} = -\frac{T}{I_{sp}g_0} \tag{7}$$

with m the spacecraft mass at time t, T the thrust level, I_{sp} the engine specific impulse in vacuum, and g_0 the reference sea-level gravitational acceleration. These equations can be modified to allow the true longitude as an independent variable as follows [40],

$$\frac{\mathrm{doe}}{\mathrm{d}L} = \frac{\mathrm{doe}}{\mathrm{d}t}\left(\frac{\mathrm{d}L}{\mathrm{d}t}\right)^{-1} \tag{8}$$

$$\frac{\mathrm{d}m}{\mathrm{d}L} = \frac{\mathrm{d}m}{\mathrm{d}t}\left(\frac{\mathrm{d}L}{\mathrm{d}t}\right)^{-1} \tag{9}$$

$$\frac{\mathrm{d}t}{\mathrm{d}L} = \left(\frac{\mathrm{d}L}{\mathrm{d}t}\right)^{-1} \tag{10}$$

with œ an orbital element. These equations were integrated using the validated high-accuracy Adams-Bashforth-Moulton (ABM) integrator from DLR's German Space Operations Centre (GSOC) flight dynamics libraries, which is a multistep method that needs to be restarted across discontinuities. This means that the method cannot be used through the thrust chattering phenomenon described by [30].

B. Q-Law Formulation

The general form of the candidate Lyapunov function presented by [1] is given by (11).

$$Q = (1 + W_P P) \sum_{œ} W_{œ} S_{œ} \left[\frac{\mathrm{d}(œ, œ_T)}{\dot{œ}_{xx}}\right]^2 \qquad (11)$$

Where Q is called the proximity quotient and is a measure of the distance between the current and target orbital elements, W_P and $W_{œ}$ are the weights of the control law, $œ_T$ is a target value of an orbital element, $\mathrm{d}(œ, œ_T)$ is the difference between the current and target orbital elements, and $\dot{œ}_{xx}$ is the maximum rate of change of the orbital element achievable in the current orbit with an optimal thrust direction. Following, P is a minimum pericentre altitude penalty function given by,

$$P = \exp\left(k_p \left(1 - \frac{r_p}{r_{p,min}}\right)\right) \qquad (12)$$

and $S_{œ}$ is a scaling function ensuring that the semi-major axis does not tend to infinity, being formulated as,

$$S_{œ} = \begin{cases} \left[1 - \left(\frac{a - a_T}{m_s a_T}\right)^{n_s}\right]^{\frac{1}{r_s}} & if\ œ = \text{a or p} \\ 1 & otherwise \end{cases} \qquad (13)$$

where m_s, n_s, r_s and k_p are user-defined constants, r_p is the spacecraft pericentre radius, $r_{p,min}$ is the user-defined minimum pericentre radius, and a is the orbit semi-major axis.

An analytical solution for the optimal thrust direction yielding the fastest decrease of Q was provided by [30]. However, various formulations using different sets of orbital elements have been suggested based on (11) [1, 29-31]. In this work, the semi-major axis augmented MEE formulation of the Q-Law presented by [30] is used without its coasting mechanism (minimum-time trajectories). Additionally, the PIKAIA genetic optimiser was used to select the $W_{œ}$ weights of the law [41], permitting to significantly improve the trajectory obtained from the Q-Law. This also permits to reject sets of weights resulting in thrust chattering before convergence to the target orbit [30].

C. Predictor-Controller Approach

A major drawback of the Q-Law is its inability to target a specific position in the target orbit. This could be desired to target a slot in the final orbit, as is usually done for GEO satellites, or to rendezvous with a spacecraft. When the Q-Law is used as an initial guess for a local optimisation algorithm, the absence of this functionality renders the initial guess rather poor for cases requiring a constraint on the final position. This results from the estimated time of flight and mass being inaccurate but also because the trajectory is not initially constraint compliant, thus resulting in no or a slower convergence of the optimiser. This limitation of the law was addressed by generalising the GEO longitude targeting method presented by [2] to be compatible with the Q-Law and for arbitrary transfers between two bounded orbits. First, the derivation of the algorithm presented by [2] is repeated to better outline the key assumptions to be relaxed for the generalisation. Then, it is generalised to circular target orbits. At last, the generalisation is extended to eccentric target orbits.

For each case, the elements of the desired position in the target orbits are propagated (from a specified epoch) and tabulated before the Q-Law propagation, such that the state vector (in MEE) can be interpolated at any timestamp. This provides a method to aim for a specific position in the target orbit which is compatible for both GEO and LEO.

GEO Case

As the final position in the target orbit heavily depends on the semi-major axis history, [2] presented a proportional controller approach to target a specific geographical longitude λ in GEO, by slightly shifting the target semi-major axis throughout the trajectory. A predictor-controller function is evaluated at a certain time interval (t_{int}) after a portion of the transfer is achieved (t_{start}), based on a specified controller gain α. The function predicts the final phase error $\Delta\Phi$ by independently propagating the trajectory using the classical Q-Law until convergence with the target orbit, and adapts the target semi-major axis using a proportional controller. This concept lies at the heart of all algorithms presented in this work.

The original algorithm was designed for geostationary target orbits, meaning that it is based on three main assumptions [2]: the target orbit is circular ($e_T = e_{GEO} \approx 0$), the target semi-major axis is $a_T = a_{GEO} = 42{,}164.14$ km, and the target inclination is $i_T = i_{GEO} = 0°$. These assumptions permit to use the geographical longitude to compute the phase error as it is constant for a given orbital position, yielding a constant phase error throughout the orbit. This permits to write,

$$\frac{\mathrm{d}\delta\lambda}{\mathrm{d}t} = n - n_{ref} \qquad (14)$$

where $\Delta\Phi = \delta\lambda = \lambda_T - \lambda$ is the difference in geographical longitude between the target slot and the spacecraft at convergence to the target orbit, $n = \sqrt{\mu/{a_t}^3}$ is the mean motion in the orbit targeted by the Q-Law, and n_{ref} is the mean motion in the desired orbit (here GEO). At the end of the transfer, by definition $\frac{\mathrm{d}\delta\lambda}{\mathrm{d}t} = 0$ as the spacecraft should have converged to the target slot [2]. Reference [2] then devised a controller,

$$\frac{\mathrm{d}\delta\lambda}{\mathrm{d}t} = -K\delta\lambda \tag{15}$$

where $K > 0$ is the controller gain. Combining (14) and (15) yields,

$$\begin{aligned} & n - n_{ref} = -K\delta\lambda \\ \Leftrightarrow & \sqrt{\frac{\mu}{a_t^3}} - \sqrt{\frac{\mu}{a_{ref}^3}} = -K\delta\lambda \\ \Leftrightarrow & a_t = \left(a_{ref}^{-3/2} - \frac{K\delta\lambda}{\sqrt{\mu}}\right)^{-2/3}. \end{aligned} \tag{16}$$

Equation (16) is used to update the target semi-major axis at each call of the predictor-controller stage, thereby changing the element evolution. As $\delta\lambda$ reduces, $a_T \to a_{geo}$, permitting to converge to GEO at the desired geographical longitude. To further enhance the reactivity of the algorithm, the gain K is dependent on the remaining time to convergence T_r (in seconds) as follows [2],

$$K = \frac{\alpha}{T_r} \tag{17}$$

where α is a user-specified gain. In theory, using $\alpha = 1, 3, 7$ permits to correct 63%, 95% and 99.9% of the initial phase error within one revolution [2]. However, in practice, numerical errors and overshooting are avoided by using,

$$K = \min\left(\frac{\alpha}{T_r}, K_{max}\right) \tag{18}$$

with $K_{max} = 10^{-4}$. Furthermore, to ensure convergence to the right inertial state vector, all elements but the argument of pericentre ω and Right Ascension of the Ascending Node Ω (RAAN) (as they are undefined for GEO) should be targeted during the propagation.

Algorithm Generalisation

The assumptions on the target orbit eccentricity and semi-major axis from [2] permit to derive a phase error formulation, that remains constant throughout the orbit if no perturbing accelerations are applied, using the geographical longitude. This behaviour is desired as it allows a smooth convergence of the controller. A similar behaviour can then be obtained using different phase angle formulations for general circular and eccentric target orbits. This results in the generalisation of (16) to,

$$a_t = \left(a_{geo}^{-3/2} - \frac{K\Delta\Phi}{\sqrt{\mu}}\right)^{-2/3} \tag{19}$$

First considering equatorial circular orbits, both the ascending node and argument of pericentre are undefined, therefore the inertial longitude λ_I is used to evaluate the phase error. This comes back to the GEO case, but the inertial longitude will be varying linearly with time throughout the orbit for a given orbital position (rather than staying constant), meaning that $\Delta\Phi = \lambda_{I_T} - \lambda_I$ remains constant for two given unperturbed orbital positions. Therefore, $\frac{\mathrm{d}\lambda_I}{\mathrm{d}t} = n$ and $\frac{\mathrm{d}\lambda_{I_{ref}}}{\mathrm{d}t} = n_{ref}$, yielding,

$$\frac{\mathrm{d}\left(\lambda_I - \lambda_{I_{ref}}\right)}{\mathrm{d}t} = n - n_{ref} \tag{20}$$

and the rest of the derivation remains the same, except that n_{ref} refers to the target orbit rather than GEO. Similarly, in circular but inclined orbits, the RAAN is defined, but the argument of the pericentre is not. This allows to use the argument of latitude, u, being the phase angle measured in the direction of motion and from the ascending node to the spacecraft, which also varies linearly through the circular orbit and $\Delta\Phi = u_T - u$ remains constant throughout the orbit for two given unperturbed orbital positions. Therefore, $\frac{\mathrm{d}u}{\mathrm{d}t} = n$ and $\frac{\mathrm{d}u_{ref}}{\mathrm{d}t} = n_{ref}$, yielding,

$$\frac{\mathrm{d}(u - u_{ref})}{\mathrm{d}t} = n - n_{ref} \tag{21}$$

and the rest of the derivation remains the same. To ensure convergence to the inertial state vector for the circular case, all elements but ω should be targeted (nor Ω for equatorial circular orbits).

For eccentric orbits, the argument of pericentre is defined and the mean anomaly can be used. As M can be related to the percentage of the orbit which was covered since the last pericentre passage, it always varies linearly. M can then be expressed as,

$$M = n(t - \tau) \tag{22}$$

where τ is the time of the last pericentre passage. It is then clear that M varies linearly throughout the orbit (n and τ are constants for a given bounded orbit), therefore $\Delta\Phi = M_T - M$ remains constant for two unperturbed orbital positions. Therefore, $\frac{\mathrm{d}M}{\mathrm{d}t} = n$ and $\frac{\mathrm{d}M_{ref}}{\mathrm{d}t} = n_{ref}$, yielding,

$$\frac{\mathrm{d}(M - M_{ref})}{\mathrm{d}t} = n - n_{ref} \tag{23}$$

Tab. 1. Reference transfers used to test the circular and eccentric orbit sixth-element targeting algorithms. All transfers employ a satellite with an initial mass of $m_0 = 2000.0$ kg and use a specific impulse of $I_{sp} = 1700.0$ s.

Case	Orbit	a [km]	e [-]	i [deg]	ω [deg]	Ω [deg]	M [deg]	T [N]
A (SSO Circular Raise)	Init.	7078.0	0.0075	97.55	55.64	90.0	0.0	0.25
	Targ.	7278.0	0.000	97.40	55.64	90.0	0.0	
	Tolerance	1	0.0001	0.001	0.001	0.001	1	
B (SSO Elliptic Raise)	Init.	7078.0	0.0075	97.55	55.64	90.0	0.0	0.5
	Targ.	7278.0	0.1	97.40	55.64	90.0	0.0	
	Tolerance	1	0.001	0.001	0.001	0.001	1	
C (Highly Eccentric)	Init.	9222.7	0.2	0.573	0.0	0.0	120.0	1.5
	Targ.	30000.0	0.7	0.573	0.0	0.0	120.0	
	Tolerance	25	0.001	0.001	1	0.001	1	

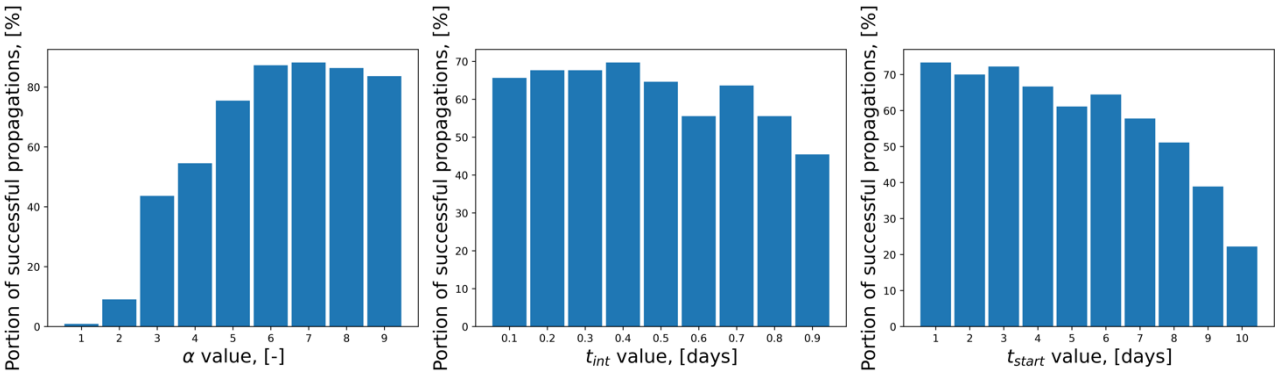

Fig. *1. Percentage of successful propagations with respect to start time, interval time, or α for case A.*

and the rest of the derivation remains the same. The use of the mean anomaly for mean motion control was already presented by Naasz [42] for different control laws. Furthermore, to ensure convergence to the same inertial position and velocity, all other orbital elements should also be targeted (except the Ω in case the inclination is zero).

III. Results

A. Test Cases

The three orbital transfers inspired from [27] and shown in Tab. 1 were considered to demonstrate the capabilities of the presented algorithms. The capabilities of the GEO longitude targeting algorithm were demonstrated by [2] and will not be considered. It is only reported that the GEO algorithm converged in 90% of the combinations considered. Note that in all cases, the mean anomaly specified for the target orbit in Tab. 1 relates to the starting epoch. Therefore, as mentioned above, the target position in the final orbit is propagated and its position is tabulated before the Q-Law propagation. The phase angle ΔΦ is then obtained by considering the position of the target slot at the time of spacecraft convergence to the target orbit, based on the tabulated data. This permits to rendezvous with a moving target.

For each transfer considered, numerous combinations of the three user-defined parameters of the sixth-element targeting algorithm (t_{start}, t_{int}, and α) were tested to illustrate their influence on the algorithm dependence. While some combinations yield transfer performances very close to the original Q-Law, others result in no convergence. Furthermore, the W_{oe} weights in (11) were selected by optimising the same trajectory using the PIKAIA genetic optimiser but without sixth-element targeting capabilities to limit the computational load.

B. Circular Target Orbits

The capability of the algorithm for the circular case was tested based on case A from Tab. 1. A parametric analysis using the ranges $\alpha = 1, 2, \ldots, 9$, $t_{start} = 0, 1, 2, \ldots, 10$ days, and $t_{int} = 0.1, 0.2, \ldots, 1.0$ days was considered. Starting the controller from the start of the propagation and evaluating it every 0.4 days with a gain of $\alpha = 9$ was found to yield the best performance with a 1.03% increase in propellant consumption compared to the same transfer without targeting. However, only 60% of the combinations considered resulted in a convergence of the trajectory. This is illustrated in Fig. 1, showing that the algorithm showed a better convergence for larger values of α and smaller t_{start}.

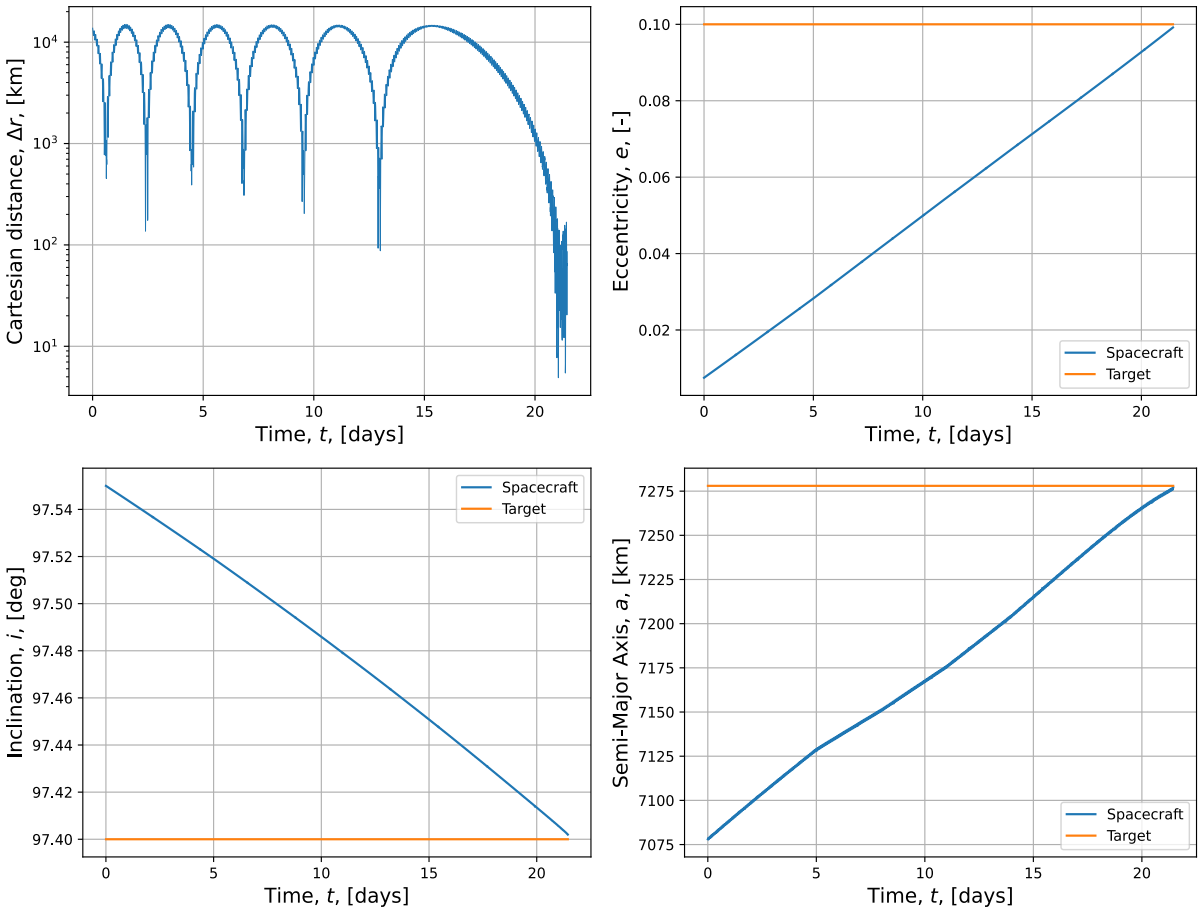

Fig. *2. Time evolution of the Cartesian distance between the target slot and the spacecraft (upper left), as well as the eccentricity (upper right), inclination (lower left), and (lower right) semi-major axis of the spacecraft and target slot over the duration of the best sixth-element targeting case B transfer.*

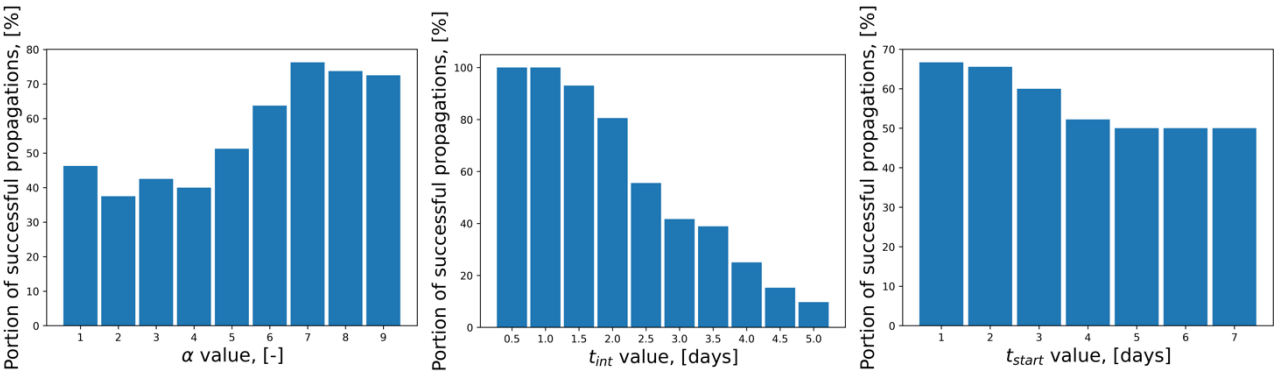

Fig. *3. Percentage of successful propagations with respect to start time, interval time, or α for case B.*

C. Eccentric Target Orbits

Cases with both low and high eccentricity were considered with cases B and C. While the majority of the combinations considered resulted in convergence to the correct target orbit and orbital slot, similarly to case A, 40% of these did not converge due to the onset of thrust chattering.

For the Case B (SSO Elliptic Raise), a parametric analysis using the ranges $\alpha = 1, 2, \ldots, 9$, $t_{start} = 1, 2, \ldots, 8$ days, and $t_{int} = 0.5, 1.0, \ldots, 5.0$ days was considered. Starting the controller after 5 days of transfer and evaluating every 3 days with a gain of $\alpha = 9$ was found to yield the best performance with only a 0.22% increase in propellant consumption compared to the same transfer without targeting. The time evolution of the distance to the target slot, and of selected

Keplerian orbital elements for this transfer are shown in Fig. 2. Furthermore, Fig. 3 shows that the time interval between evaluations of the predictor-controller stage has the largest influence on the convergence of the algorithm. This is expected, as the controller is not called enough times to ensure a smooth convergence when the interval time is too large. Additionally, it appears that higher values of α result in a more reliable convergence for this transfer.

For the Case C transfer, the ranges $\alpha = 1, 2, \dots, 9$, $t_{start} = 0, 3, 6, \dots, 18$ days, and $t_{int} = 1, 2, \dots, 5$ days were considered heuristically and the best combination of parameters found starts the controller at the start of the propagation ($t_{start} = 0$ days) with an interval of 3 days and $\alpha = 6$, yielding a 0.25% propellant mass increase to target the specific slot. This rendezvous transfer is shown in Fig. 4, correctly inserting in the target orbit at the desired position. Furthermore, Fig. 5 indicates that larger values of α result in a better convergence, and lower value of t_{int} are preferred, similarly to cases A and B.

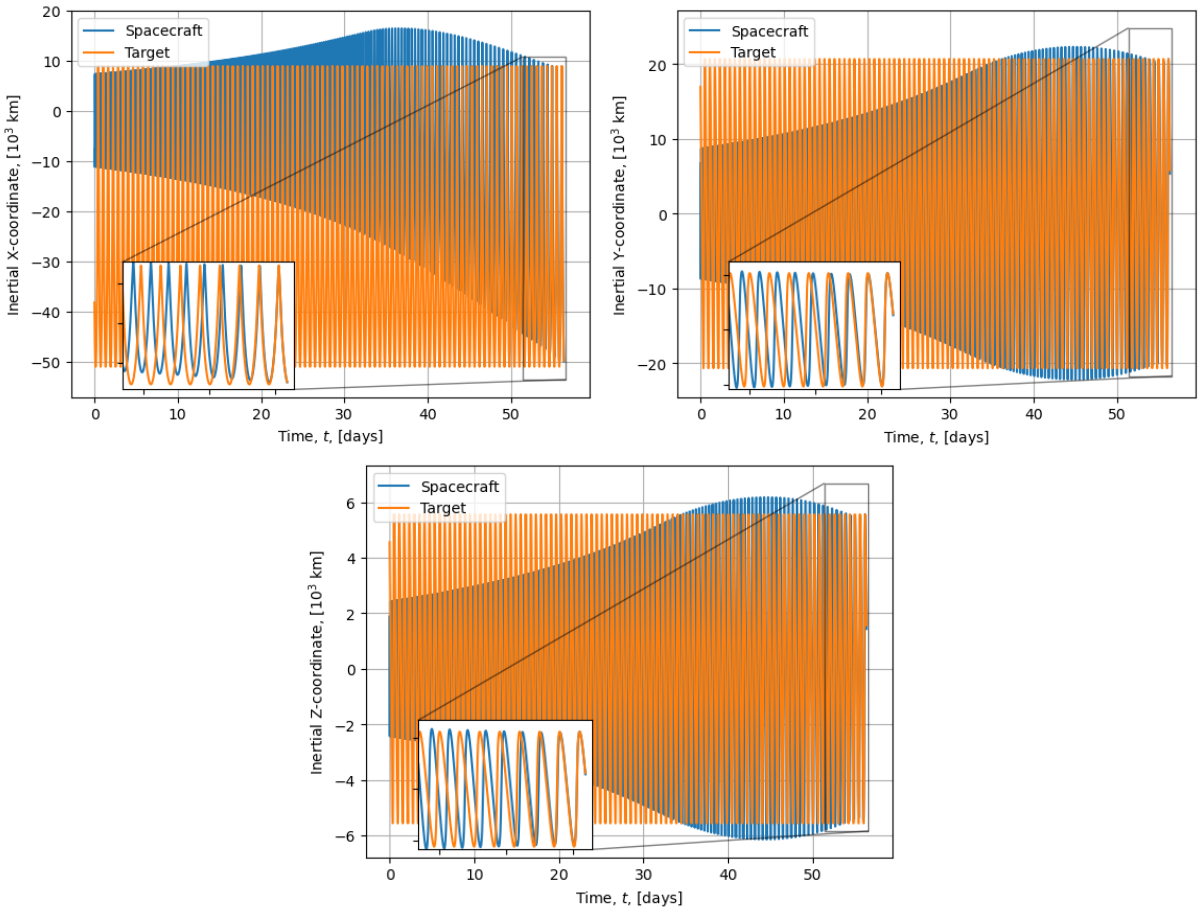

Fig. *4. Cartesian coordinates of the spacecraft and target slot as a function of time during the Case C transfer.*

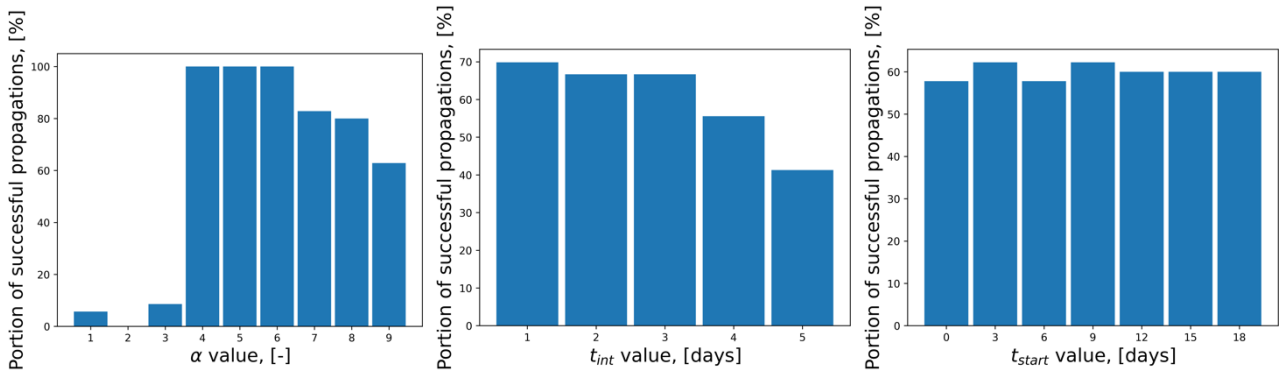

Fig. *5. Percentage of successful propagations for start time, interval time, or α in the Case C transfer.*

IV. Discussion

The presented predictor-controller approach enabling sixth-element targeting functionality to the Q-Law was found to yield promising results. Certain combinations of t_{start}, t_{int}, and α yield convergence to the desired orbital slot with a minimal impact on the propellant consumption. However, 40% of the combinations do not converge for both the circular and eccentric cases because of thrust chattering, compared to only 10% for the GEO algorithm. As this phenomenon is characterised by very fast changes in the optimal thrust direction obtained from the Q-Law, the integrator gets stuck, and the propagation cannot be continued. While the use of a fixed-step integrator could push through the thrust chattering phenomenon until convergence, this would result in inaccurate estimates of $\Delta\Phi$ in the predictor stage and prohibit the convergence of the targeting algorithm.

From the combinations which did converge, it can be observed that smaller values of t_{start} *and* t_{int} yield a better convergence. This is expected, as both yield a smoother behaviour of the controller and therefore smaller changes in the targeted semi-major axis at each evaluation of the predictor-controller stage. Such behaviour reduces the probability of thrust chattering, and therefore increases the convergence rate. However, this results in an increased computational load. Furthermore, while higher α-gain values were found to benefit the convergence of the algorithm, adequate values are case-dependent and need to be assessed for each transfer separately. Additionally, the convergence of the algorithm does not automatically imply an optimal performance. However, the kind of performance analysis presented in this work only needs to be performed once for a new transfer and the obtained algorithm constants will be similar for similar transfers.

Considering the best combinations resulting from each case, test case A revealed a significantly worse drop in performance because of sixth-element targeting compared to cases B and C (1.03% against 0.22% and 0.25%). Such differences are unexpected and are unexplained at this stage, indicating that further work on the circular version of the algorithm is necessary to improve its performance. One possible explanation for this behaviour is that while the circular target orbit considered in case A does have $e_T = 0$ exactly (which is an assumption of the derivation of the method), the orbit reached at the end of the transfer has $e \approx 0.0001$ due to the specified tolerance on the eccentricity. A better performance would then be obtained with a smaller tolerance. However, [31] showed that the AMEE and MEE formulations of the Q-Law both possess a singularity at $e = 0$, meaning that exactly circular orbits cannot be targeted and further reducing the tolerance could result in a trajectory encountering the singularity. Nevertheless, the availability of a sixth-element targeting method for arbitrary circular orbits remains valuable, even if suboptimal, to be used as an initial guess of a local optimisation algorithm.

V. Conclusion

This work presented and demonstrated the capability of a sixth-element targeting algorithm for the Q-Law applicable to any bounded target orbit. The method is a generalisation of the work from [2] and relies on the evaluation of a predictor-controller stage which evaluates the final phase error between the desired target slot and the spacecraft at convergence with the target orbit, and adapts the semi-major axis evolution to reduce the error. The algorithm convergence and performance depend on three user-specified constants: an α controller gain, the epoch at which it is started, and the frequency at which it is evaluated throughout the transfer. The capability of the algorithm was demonstrated based on three test cases and results in a minimal increase in fuel mass used compared to the classical Q-Law for eccentric orbits. However, the method applied for circular orbit shows a larger drop in performance which should be further investigated. Further work shall include improving the circular version of the method, testing the algorithm performance in a perturbed environment with eclipsing (and coast phases), and developing the Q-Law to reliably avoid thrust chattering. The latter is not a problem specific to the proposed method, but improving this general issue would aid in designing more complex transfers. Additionally, a genetic optimiser could be used to select the three user-defined functions, rather than the parametric analyses presented in this work. This would permit to directly exclude combinations which encounter thrust chattering and improve the rendezvous trajectory optimality. However, the computational time linked to an excessive number of calls to the predictor-controller stage needs to be considered in this case.

Despite the reported future improvements, the proposed method already opens the door to fast rendezvous mission design and significantly improves the initial guess quality for further trajectory optimisation.

VI. References

[1] Petropoulos, Anastassios E. "Simple control laws for low-thrust orbit transfers.", *AAS/AIAA Astrodynamics Specialists Conference*, Montana, USA, 2003.

[2] S. Locoche, K. Lagadec, S. Erb, and C.Y. Vallès, "Reducing operation cost with autonomous guidance for electrical orbit raising," *8th international conference on astrodynamics tools and techniques (ICATT)*, 2021.

[3] R.H. Goddard, *R. H. Goddard: An Autobiography*, Robert H. Goddard Notebook dated September 6, 1906.

[4] E. Stuhlinger, *Ion propulsion for space flight*, McGraw-Hill New York, 1964.
[5] E. Stuhlinger, “Electric space propulsion systems,” *Space Science Reviews*, vol. 7, no. 5, pp. 985-847, 1967.
[6] L. Garrigues and P. Coche, "Electric propulsion: comparisons between different concepts," *Plasma Physics and Controlled Fusion*, vol. 53, no.12, 2011.
[7] D. Lev, R.M. Myers, K.M. Lemmer, J. Kolbeck, H. Koizumi and K. Polzin, “The technological and commercial expansion of electric propulsion,” *Acta Astronautica*, vol. 159, pp. 213-227, 2019.
[9] D.F. Lawden, “Impulsive Transfer between Elliptical Orbits,” in *Mathematics in Science and Engineering*, vol. 5, pp. 323-351, 1962.
[10] N.X. Vinh and S.H. Kuo and C. Marchal, “Optimal time-free nodal transfers between elliptical orbits,” *Acta Astronautica*, vol. 18, no. 8, pp. 875-880, 1988.
[11] J. E. Prussing and J-H. Chiu, “Optimal multiple-impulse time-fixed rendezvous between circular orbits,” *Journal of Guidance, Control, and Dynamics*, vol. 9, no. 1, pp. 17-22, 1986.
[12] D. J. Jezewski and H. L. Rozendaal, “An efficient method for calculating optimal free-space n-impulse trajectories,” *AIAA Journal*, vol. 6, no. 11, pp. 2160-2165, 1968.
[13] O. Abdelkhalik and D. Mortari, “N-impulse orbit transfer using genetic algorithms,” *Journal of Spacecraft and Rockets*, vol. 44, no. 2, pp. 456-460, 2007.
[14] D. Morante, M. Sanjurjo Rivo and M. Soler, “A Survey on Low-Thrust Trajectory Optimization Approaches,” *Aerospace*, vol. 8, no. 3, p. 88, 2021.
[15] A. E. Petropoulos and J. A. Sims, “A review of some exact solutions to the planar equations of motion of a thrusting spacecraft,” 2002.
[16] J. T. Betts, “Survey of Numerical Methods for Trajectory Optimization,” *Journal of Guidance, Control, and Dynamics*, vol. 21, no. 2, pp. 193-207, 1998.
[17] A. V. Rao, “A survey of numerical methods for optimal control,” *Advances in Astronautical Sciences*, vol. 135, no. 1, pp. 497-528, 2009.
[18] B. A. Conway, “A survey of methods available for the numerical optimization of continuous dynamic systems,” *Journal of Optimization Theory and Applications*, vol. 152, pp. 271-306, 2012.
[19] A. Shirazi, J. Ceberio and J. A. Lozano, “Spacecraft trajectory optimization: A review of models, objectives, approaches and solutions,” *Progress in Aerospace Sciences*, vol. 102, pp. 76-98, 2018.
[20] Y. Dalin, X. Bo and G. Youtao, “Optimal strategy for low-thrust spiral trajectories using Lyapunov-based guidance,” *Advances in Space Research*, vol. 56, no. 5, pp. 865-878, 2015.
[21] O. Von Stryk and R. Bulirsch, “Direct and indirect methods for trajectory optimization,” *Annals of operations research*, vol. 37, pp. 357-373, 1992.
[22] P. Coppens, B. Hermans, J. Vandersteen, G. Pipeleers and P. Patrinos, “A New Heuristic Approach for Low-Thrust Spacecraft Trajectory Optimization,” *IFAC-PapersOnLine*, vol. 52, no. 2, pp. 6490-6495, 2020.
[23] C. Pukdeboon, “A review of fundamentals of Lypunov theory,” *Journal of Applied Science*, vol. 10, no. 2, 2011.
[24] M. R. Ilgen, “Low thrust OTV guidance using Lyapunov optimal feedback control techniques,” in *AAS/AIAA Astrodynamics Specialists Conference*, pp. 613-630, 1993.
[25] D. E. Chang, D. F. Chichka and J. E. Marsden, “Lyapunov-based transfer between elliptic Keplerian orbits,” *Discrete and Continuous Dynamical Systems Series B*, vol. 2, no. 1, pp. 57-68, 2002.
[26] A. E. Petropoulos, “Simple control laws for low-thrust orbit transfers,” in *AAS/AIAA Astrodynamics Specialists Conference*, 2003.
[27] A. E. Petropoulos, “Low-thrust orbit transfers using candidate Lyapunov functions with a mechanism for coasting,” in *AIAA/AAS Astrodynamics Specialist Conference*, 2004.
[28] A. E. Petropoulos, “Refinements to the Q-law for the low-thrust orbit transfers,” in *15th AAS/AIAA Space Flight Mechanics Conference*, 2005.
[29] R. Yuan, C. Pingyuan and L. Enjie, “A low-thrust guidance law based on Lyapunov feedback control and hybrid genetic algorithm,” *Aircraft Engineering and Aerospace Technology*, vol. 79, no. 2, pp. 144-149, 2007.
[30] G. I. Varga and J. M. S. Pérez. "Many-revolution low-thrust orbit transfer computation using equinoctial Q-law including J2 and eclipse effects," in *6th International Conference on Astrodynamics Tools and Techniques*, vol. 1, pp. 29-42, 2016.
[31] S. Narayanaswaly, C. J. Damaren, “Equinoctial Lyapunov Control Law for Low-Thrust Rendezvous,” *Journal of Guidance, Control, and Dynamics*, vol. 46, no. 4, pp. 781-795, 2023.
[32] H. Holt, R. Armellin, N. Baresi, Y. Hashida, A. Turconi, A. Scorsoglio and R. Furfaro, “Optimal Q-laws via reinforcement learning with guaranteed stability,” *Acta Astronautica*, vol. 187, pp. 511-528, 2021.
[33] H. Holt, R. Armellin, A. Scorsoglio and R. Furfaro, “Low-Thrust Trajectory Design Using Closed-Loop Feedback-Driven Control Laws and State-Dependent Parameters,” in *AIAA Scitech 2020 Forum*, 2020.
[34] J. Shannon, M. Ozimek, J. Atchison and C. Hartzell, “Q-Law Aided Direct Trajectory Optimization for the High-Fidelity, Many-Revolution, Low-Thrust Orbit Transfer Problem,” *Advances in the Astronautical Sciences*, vol. 168, pp. 781-800, 2019.
[35] L. Niccolai, A. A. Quarta and G. Mengali, “ Solar sail heliocentric transfers with a Q-law,” *Acta Astronautica*, vol. 188, pp. 352-361, 2021.

[36] J. Shannon, "Selected Problems in Many-Revolution Trajectory Optimization Using Q-Law," Doctoral Dissertation, University of Maryland, College Park, 2021.
[37] D. V. Lantukh, C. L. Ranieri, M. D. DiPrinzio and P. J. Edelman, "Enhanced q-law Lyapunov control for low-thrust transfer and rendezvous design," In *2017 AAS/AIAA Astrodynamics Specialist Conference*, 2017.
[38] H. Klinkrad. *Space debris: models and risk analysis*. Springer Science & Business Media, 2006.
[39] J. T. Betts, "Optimal interplanetary orbit transfers by direct transcription," *Journal of the Astronautical Sciences*, vol. 42, no. 3, pp. 247-268, 1994.
[40] J. T. Betts and S. O. Erb, "Optimal low thrust trajectories to the moon," *SIAM Journal on Applied Dynamical Systems*, vol. 2, no. 2, pp. 144-170, 2003.
[41] P. Charbonneau and B. Knapp, "A user's guide to PIKAIA 1.0," NCAR Technical Note, TN-418-+IA, Boulder: National Center for Atmospheric Research, 1995.
[42] B. J. Naasz, "Classical element feedback control for spacecraft orbital maneuvers," Doctoral Dissertation, Virginia Tech, 2002.